Journal of Physical Sciences, Vol. 21, 2016, 167-175
ISSN: 2350-0352 (print), www.vidyasagar.ac.in/journal
Published on 24 December 2016

Structural, Optical and Optoelectrical Study of ZnS Nanoparticles by Varying Reducing Agent in Chemical Reduction Route

K. Bera, S. Saha and P. C. Jana

Department of Physics and Technophysics
Vidyasagar University, Midnapore-721102, West Bengal, India
kamal.phy87@gmail.com, sahaphys.vu@gmail.com,

Received 3 September 2016; accepted 23 November2016

ABSTRACT

In this work we report on the growth of ZnS semiconductor nanocrystals with different ratio of reducing agent using chemical reduction route in THF medium. Reducing agent takes an important role in the growth of nanoparticles as it determines the reaction rate in the formation of ZnS nanoparticle. With increased amounts of sodium borohydride as a reducing agent, the sizes of the nanoparticles are decreased. The samples are characterized using XRD, electron diffraction, electron micrograph, EDAX, optical absorption, photoluminescence techniques. XRD and TEM shows that particle size is reduced with increase of reducing agent ratio. Optical absorption study shows that band gap increases with decrease of particle size. Photoluminescence study shows that there is band edge luminescence as well as luminescence from surface states. Photoconductivity and conductivity of the films composed of ZnS nanoparticles are studied. Relaxation time is measured and is found to be dependent on the size of the nanoparticle.

Keywords: ZnS nanoparticles, Reducing agent, Microstructural properties, Optical properties, Photoluminescence Photoconductivity.

1. Introduction

Nanocrystalline semiconductor particles have attracted considerable interest over the past few years, because of their novel properties, such as large surface-to-volume ratio and the three dimensional confinement of the electrons [1-3]. The degrees of confinement of the electrons are changed due to the change of the size of the particles and hence affects the electronic structure of the solid especially the band gap edges. When the particle radius falls below the excitonic Bohr radius, the band gap energy is widened, leading to a blueshift in the band gap, emission spectra, etc. On the other hand, the surface states will play a more important role in the nanoparticles, due to their large surface-to-volume ratio with a decrease in particle size (surface effects).

Among the family of II–VI inorganic semiconductors, ZnS are the foremost candidates because of their favorable electronic and optical properties for optoelectronic applications especially in nanocrystalline form. Particle size reduction has a tremendous

effect on the properties of the ZnS such as blueshift in the optical absorption spectrum, increased luminescence, enhanced oscillator strength, nonlinear optical effects, geometrical structure, chemical bonds, ionization potential, mechanical strength, melting point, etc. ZnS can have two different crystal structures zinc blende and wurtzite[4-5], both have the same band gap energy (3.68 eV) and the direct band structure. ZnS has been extensively used for the cathode ray tube, field emission display,and scintillators as one of the most frequently used phosphors[6-8], thin-film electroluminescent devices [9], infrared windows [10], flat panel displays[11], sensors[12], lasers [13], bioanalytical labeling [14] and memristor applications[15], n window layers for solar cells[16-17], large area OLED [18].

Nanocrystalline ZnS can be prepared by various methods like sputtering[19], evaporation[20] , wet chemical[21] , sol-gel[22], sonochemical method[23], Solid state [24], micro-wave irradiation[25-26] or synthesis under high-gravity environment[27].
This paper discusses the preparation of zinc sulfide nanocrystals via a simple chemical reduction route[28] in room temperature.In this process Sodium borohydride is used as reducing agent to initiate the reaction between zinc chloride and sulphur at room temperature. Amount of reducing agent are varied to study the effect of reducing agent. The used method is cost effective and free from experimental hazards. The structural, optical and photoluminescence properties of as grown samples are characterized by XRD, TEM, SAED, EDAX, optical absorption and photoluminescence techniques. Nanofilm is also grown from the dispersed medium on glass substrate and is used for photorelaxation study. An attempt is made to correlate the result with ratio of reducing agent.

2. Experimental methods

Anhydrous $ZnCl_2$ (99.999%) (1360.8mg), sulfur powder (99.999%) (320.6mg) and stochiometric amount of sodium borohydride (98%) (378.3mg, 1134.9mg, 1891.5 mg) were purchased from Alfa-Aesar to prepare different samples. To prepare different samples the amount of ratio for $ZnCl_2$, S and $NaBH_4$ are in 1:1:1, 1:1:3, 1:1:5 respectively. Tetrahydrofuran (99%) used as capping agent. Sodium borohydride were taken to ini-tiate the reaction at 40^0C.The stirring was continued for three hours at a particular speed. For microstructural study, as prepared ZnS nanoparticles were dispersed in ethanol by ultrasonification. A small drop of this dispersed samples were placed on a thin carbon film supported on the carbon grid and kept for some time for drying. The transmission electron micro- graph (TEM) of the prepared nanoparticles was acquired using JEOL-JEM-200 operating at 200 kV. The SAED pattern and EDAX analysis of the said nanoparticles were also carried out. The XRD patterns of the said samples are obtained by using Rigaku MiniFlex-II X-ray diffractometer. The optical absorption spectrum of the samples was taken by using Shimadzu-Pharmaspec-1700 UV-VIS after ultrasonification in ethanol. The photoluminescence spectrum of the as prepared samples was obtained by using Hitachi-F7000-FL spectrophotometer. Nanofilms corresponding to samples of different reducing agent ratio are grown on glass. The samples are dispersed in ethanol using ultrasonicator. The glass slides are dipped into the dispersed medium for at least six hours. Film of ZnS is grown on the glass substrate. Graphite paint is used as ohmic contact for measurement of Conductivity and photoconductivity of nanofilms. Conductivity and photoconductivity is measured using Keithly Electrometer - 6514.Intensity of ultraviolet light falling on the sample is measured by a luxmeter.

3. Results and discussion

3.1. Structural determination (XRD)

The powder X-ray diffraction (XRD) pattern on the samples were recorded by a X-ray diffractometer (miniflex II,desktop-X-ray diffractometer) using Cu-k radiation of wave length $\lambda = 1.54\ A^0$ for 2Θ ranging from 20^0 to 80^0. The diffraction peaks of the XRD pattern of as prepared the samples are shown in Figure 1. The XRD pattern of as prepared nanoparticles exhibit the peaks at scattering angle (2θ) 28.61º, 48.07º, 56.72º corresponds to (111), (220), (311) planes respectively.

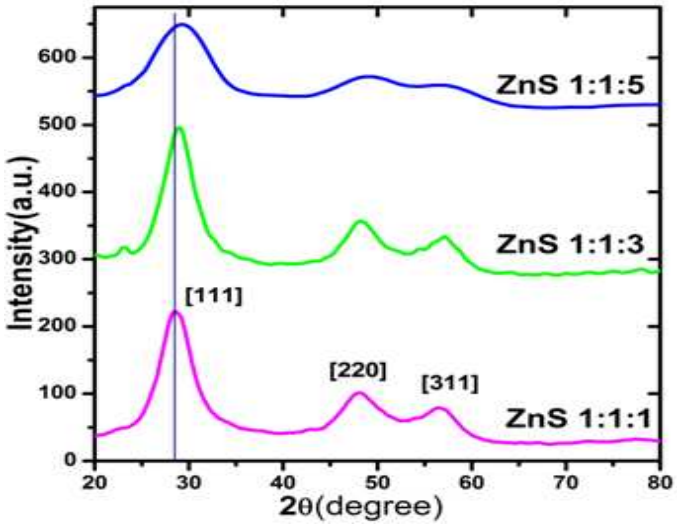

Figure 1:

Diffraction peaks of the XRD pattern of the as synthesized samples show cubic phase. The peak broadening in the X-ray diffraction (XRD) patterns of the samples shown in Figure1clearly indicates that nanocrystal size is reduced with increase of reducing agent ratio.

First peak shows maxima at value (2θ) 28.61º and is very close to the bulk value. Nanoparticles grown with increase of ratio of reducing agent gives maxima at higher (2θ) value. This clearly shows that there is increase of stacking fault probability with decrease of particle size. Shift of all the Bragg peaks means that there is possibility of increase of dislocation with increase of reducing agent ratio.

3.2 Morphological Study (TEM)

Morphologies of the products synthesized at fixed reactional time at concentration for different molar ratio of reducing agent are shown in figure 2-4.

The TEM images clearly show that the particle size depends on the ratio of reducing agent. The particle sizes of the as prepared samples decrease as increase in the ratio of reducing agent shown in table 1. The smallest particle size has observed 5 nm in case of ratio 1:1:5(Figure 4).

Figure 5 shows typical EDX of ZnS nanoparticles grown at ratio1:1:1. EDAX analysis show that the Zn:S ratio increases with increase of the ratio of reducing agent. This is probably due to the increased reduction of sulphur with increase of reducing agent

which opposes the agglomeration of the particles. As a result particle size is reduced and ratio of sulphur is decreased.

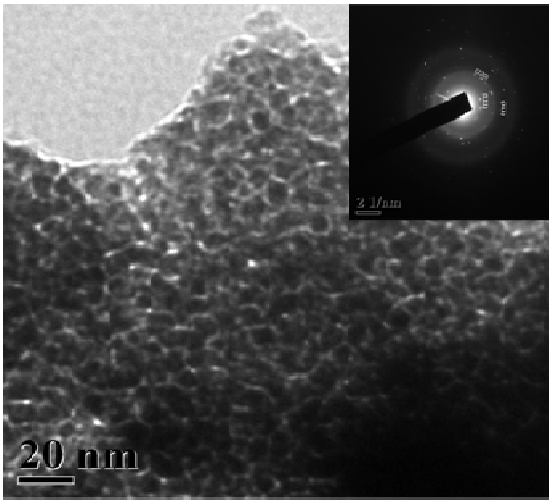

Figure 2:

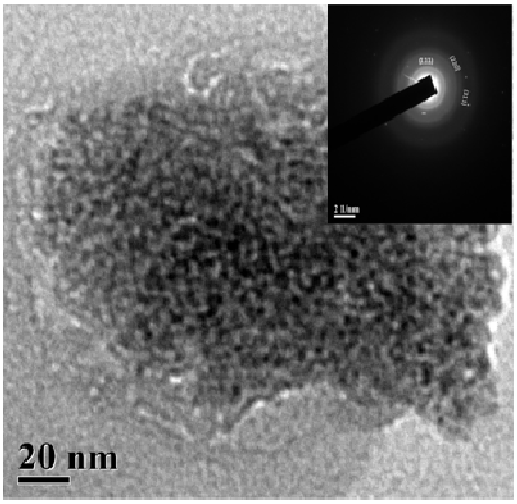

Figure 3:

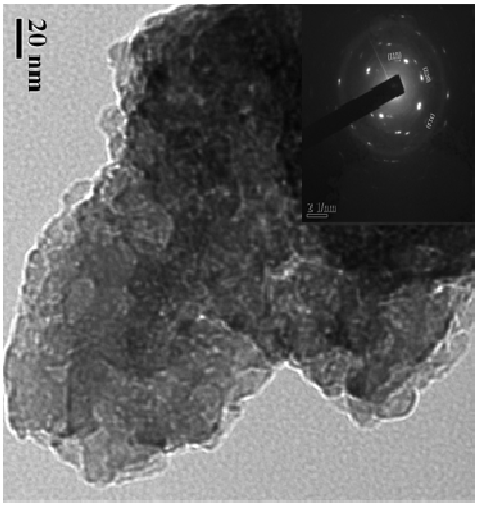

Figure 4:

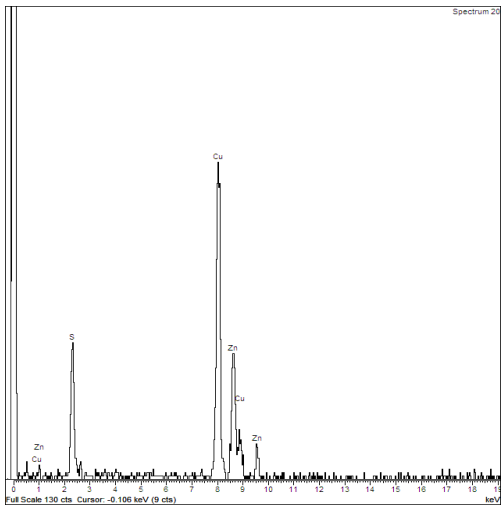

Figure 5:

3.3. Optical Properties of ZnS – Nanostructure

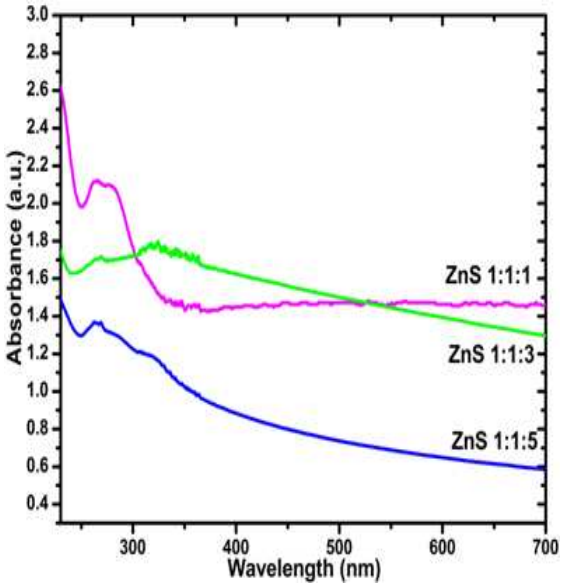

Figure 6:

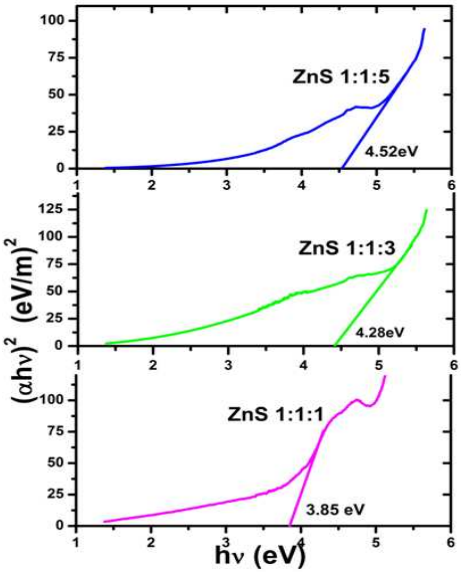

Figure 7:

Figure 6 shows the variation of optical absorbance with wavelength of the as prepared nanoparticles. Optical absorption coefficient has been calculated in the wavelength region 200–700 nm. Optical absorption coefficient (α) is calculated at each wave length.

The band gaps of the as-prepared nanoparticles are determined from the relation [29]

$$(\alpha h\nu)^2 = C(h\nu - E_g)$$

where C is a constant, E_g is the band gap of the material and α is the absorption coefficient.

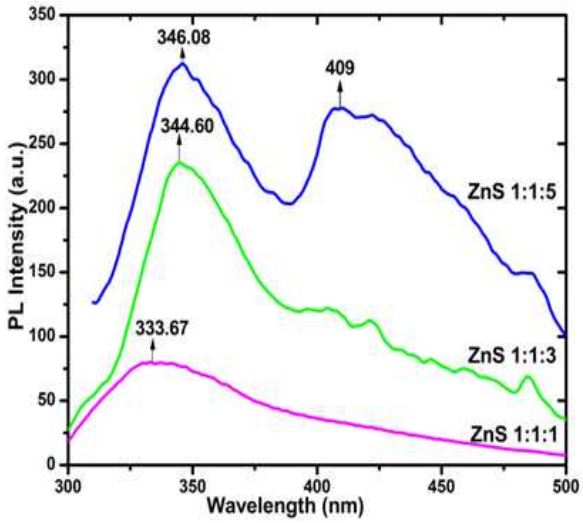

Figure 8:

Fig. 7 shows the plot of $(\alpha h\nu)^2$ vs. energy ($h\nu$) and it is used to determine band gap in each case. The band gap of as prepared samples increases as ratio increases. This means that quantum confinement takes place.

3.4. Photoluminescence

The PL spectra of the ZnS sample products were measured with excitation wavelength 266 nm.

The figure 8 shows PL spectra of the ZnS samples prepared at different ratio. With increase of reducing agent ratio PL spectra clearly indicates the appearances of new peak around 409 nm. Also peak intensity is reduced with the decrease of reducing agent ratio & finally disappears at the ratio 1:1:1. The peak around 409 nm is attributed to the surface state .The peak around 332 nm corresponding to energy 3.73 eV gives emission from a state which is closer to the band edge. This peak shifts to the higher wavelength with increase of reducing agent ratio.

3.5. Photoconductivity study

The growth of photocurrent is shown in figure 9 -11. After the steady current is reached the light is switched off. Relaxation time is measured from long time photodecay graph. The corresponding graph is displayed by the figure 9-11. Relaxation time is measured using the relation $\Delta n = \Delta ns \exp(-t/\tau)$. This relation can be correlated to experimentally measurable parameter by $\Delta n/\Delta ns = \Delta Iph(s)/\Delta Iph(t) = \exp(t/\tau)$,where $\Delta Iph(s)$ is the change of steady photo current with respect to dark current value and $\Delta Iph(t)$ is the change of photo current at any arbitrary time t with respect to the dark.

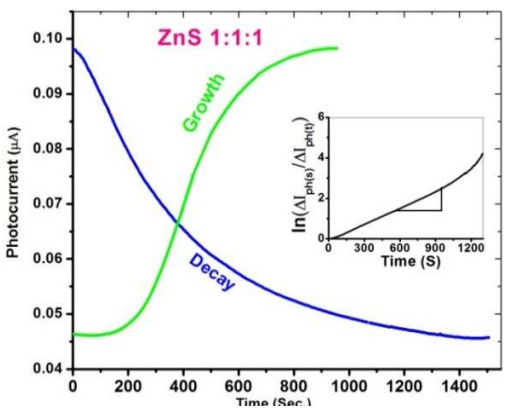

Figure 9:

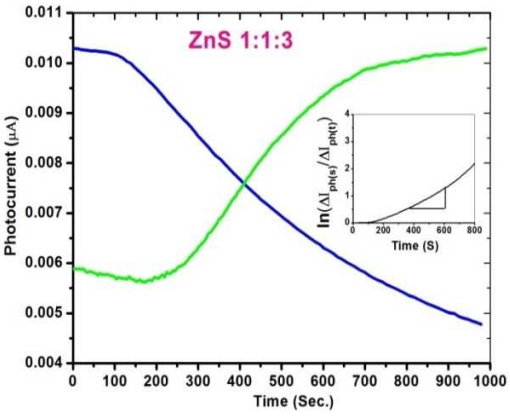

Figure 10:

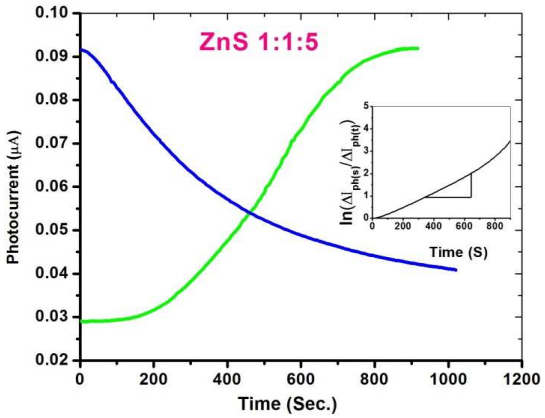

Figure 11:

The plot of ln (ΔIph(s)/ΔIph(t)) vs. t gives the straight line and is displayed in figure 9-11(inset). From the slope, the long time relaxation is estimated. Relaxation time decreases with increase of reducing agent ratio. This is probably due to the decrease of the particle size which results in the increase of surface area. As a result the surface recombination is increased and thereby relaxation time is reduced.

The slow photoconductive decay is attributed here to the reconstruction of recombination barrier which has spatially separated the photogenerated electron-hole pairs by trapping minority carriers. The dark conductivity is established only after equilibrium filling of the recombination barrier states.The exponential decay shows that recombination barrier height does not change at all under illumination & this is the case under weak illumination.

4. Conclusions

ZnS is prepeared in a cost effective way and characterized structurally, optically and electrically. The effect of reducing agent i.e $NaBH_4$ is prominent in the formation of nanoparticles. XRD and TEM indicate that with increase of reducing agent particle size is reduced. As a result band gap is blue shifted. PL spectra clearly show the appearance of the peak due to surface state for samples grown with increased reducing agent ratio. The effect of particle size on long time relaxation is evident due to the involvement of surface recombation. Variation of characteristics of ZnS nanoparticles with change in reducing agent are shown in table 1.

Table1: Summarisation table

Sample Name	PL Peak (nm)		Band Gap (eV)	Particle Size (nm)	EDAX %
Zns 1:1:1	333.67		3.85	10	Zn- 51.56 S- 48.44
ZnS 1:1:3	344.60	408	4.28	7	Zn- 60.02 S---39.98
ZnS 1:1:5	346.08	409	4.52	5	Zn – 72.91 S- 27.08

Acknowledgements: Authors are acknowledging UGC and DST for their constant support to Physics department of Vidyasagar University through SAP and FIST programme respectively.

REFERENCES

1. Y.Wang and N.Herron, Nanometer-sized semiconductor clusters: materials synthesis, quantum size effects, and photophysical properties, *The Journal of Physical Chemistry*, 95 (1991) 525-532.
2. H.Weller, Quantized semiconductor particles: a novel state of matter for materials science, *Advanced Materials*, 5 (1993) 88–95.
3. A.P.Alivisatos, Semiconductor clusters, nanocrystals, and quantum dots, *Science*, 271(1996) 933.
4. Z.Deng, J.Qi, Y.Zhang, Q.Liao and Y.Huang, Growth mechanism and optical properties of ZnS nanotetrapods, *Nanotechnology*, 18 (2007) 475603.
5. S.Senthilkumaar, and R.T.Selvi, Formation of hexagonal shaped wurtzite zinc sulphide nano rods, *Applied Physics A*, 94 (2009) 123-129.
6. H.Okuda, J.Takada, Y.Iwasaki, N.Hashimoto and C.Nagao, A new 9" projection CRT, with dichroic coating for HDTV, *IEEE Transactions on Consumer Electronics*, 36 (1990) 436-443.
7. J.Ghrayeb, T.W.Jackson, R.Daniels and D.G.Hopper, Review of field emission display potential as a future (leap-frog) flat panel technology, *In AeroSense* '97, (1997) 237-248.
8. J.C.Barton, and P.W.Ranby, Zinc sulphide scintillator with faster decay, *Journal of Physics E Scientific Instruments*, 10 (1977) 437.
9. S.Tiwari, S.Tiwari, and B.P.Chandra, Characteristics of ac electroluminescence in thin film ZnS: Mn display devices, *Journal of Materials Science: Materials in Electronics*, 15 (2004) 569-574.
10. A.R.Hilton, Infrared transmitting materials, *Journal of Electronic Materials*, 2 (1973) 211-225.
11. X.Liu, X.Cai, J.Mao and C.Jin, ZnS/Ag/ZnS nano-multilayer films for transparent electrodes in flat display application, *Applied Surface Science*, 183 (2001) 103-110.
12. X.Wang, Z.Xie, H.Huang, Z.Liu, D.Chen and G.Shen, Gas sensors, thermistor and photodetector based on ZnS nanowires, *Journal of Materials Chemistry*, 22 (2012) 6845-6850.
13. A.Z.Obidin, A.N.Pechenov, Y.M.Popov, V.A.Frolov, Y.V.Korostelin and P.V.E.Shapkin, Streamer zinc sulfide laser, *Soviet Journal of Quantum Electronics*, 18 (1988) 1100.
14. J.Riegler and T.Nann, Application of luminescent nanocrystals as labels for biological molecules, *Analytical and bioanalytical chemistry*, 379 (2004) 913-919.
15. R.Bhadra, V.N.Singh, B.R.Mehta and P.Datta, Studies on some aspects of ZnS nanocrystals for possible applications in electronics, *Chalcogenide Letters*, 6 (2009) 189-196.

16. I.O.Oladeji and L.Chow, Synthesis and processing of CdS/ZnS multilayer films for solar cell application, *Thin Solid Films,* 474 (2005) 77-83.
17. R.Menner, B.Dimmler, R.H.Mauch and H.W.Schock, II--VI compound thin films for windows in heterojunction solar cells, *Journal of crystal growth,* 86 (1988) 906-911.
18. M.Sajid, M.Zubair, Y.H.Doh, K.H.Na and K.H.Choi, Flexible large area organic light emitting diode fabricated by electrohydrodynamics atomization technique, *Journal of Materials Science: Materials in Electronics,* 26 (2015) 7192-7199.
19. D.H.Hwang, J.H.Ahn, K.N.Hui, K.San Hui and Y.G.Son, Structural and optical properties of ZnS thin films deposited by RF magnetron sputtering, *Nanoscale research letters,* 7 (2012) 1-7.
20. S.Velumani and J.A.Ascencio, Formation of ZnS nanorods by simple evaporation technique, *Applied Physics A,* 79 (2004) 153-156.
21. H.Li, B.Zhu, Y.Feng, S.Wang, S.Zhang and W.Huang, Preparation of TiO2/ZnS core/sheath heterostructure nanotubes via a wet chemical method and their photocatalytic activity, *Reaction Kinetics and Catalysis Letters,* 92 (2007) 239-246.
22. B.Bhattacharjee, D.Ganguli, S.Chaudhuri and A.K.Pal, Synthesis and optical characterization of sol--gel derived zinc sulphide nanoparticles confined in amorphous silica thin films, *Materials Chemistry and Physics,* 78 (2003) 372-379.
23. G.H.Wang, B.Y.Geng, X.M.Huang, Y.W.Wang, G.H.Li and L.D.Zhang, A convenient ultrasonic irradiation technique for in situ synthesis of zinc sulfide nanocrystallites at room temperature, *Applied Physics A,* 77 (2003) 933-936.
24. H.Y.Lu, S.Y.Chu and S.S.Tan, The characteristics of low-temperature-synthesized ZnS and ZnO nanoparticles, *Journal of Crystal growth,* 269 (2004) 385-391.
25. Y.Zhao, J.M.Hong and J.J.Zhu, Microwave-assisted self-assembled ZnS nanoballs, *Journal of crystal growth,* 270 (2004) 438-445.
26. A.V.Murugan, O.Y.Heng, V.Ravi, A.K.Viswanath and V.Saaminathan, Photoluminescence properties of nanocrystalline ZnS on nanoporous silicon, *Journal of materials science,* 41 (2006) 1459-1464.
27. J.Chen, Y.Li, Y.Wang, J.Yun and D.Cao, Preparation and characterization of zinc sulfide nanoparticles under high-gravity environment, *Materials Research Bulletin,* 39 (2004) 185-194.
28. W.Wang, I.Germanenko and M.S.El-Shall, Room-temperature synthesis and characterization of nanocrystalline CdS, ZnS, and Cd x Zn1-x S, *Chemistry of Materials,* 14 (2002) 3028-3033.
29. P.S.Kireev, *Semiconductor Physics,* Mir Publishers, 2nd edn (1968) 545.